

EUR 4863 e

COMMISSION OF THE EUROPEAN COMMUNITIES

**POST-IRRADIATION EXAMINATION
OF THE FUEL ROD CART-C1 N° 4**

by

A. FRIGO, R. KLERSY, K.H. SCHRADER, A. SCHÜRENKÄMPER
(EURATOM)
A. BENVENUTI, G. CAMONA and F. MANTEGA
(CISE)

1972



Joint Nuclear Research Centre
Ispra Establishment - Italy

LEGAL NOTICE

This document was prepared under the sponsorship of the Commission of the European Communities.

Neither the Commission of the European Communities, its contractors nor any person acting on their behalf:

make any warranty or representation, express or implied, with respect to the accuracy, completeness, or usefulness of the information contained in this document, or that the use of any information, apparatus, method or process disclosed in this document may not infringe privately owned rights; or

assume any liability with respect to the use of, or for damages resulting from the use of any information, apparatus, method or process disclosed in this document.

This report is on sale at the addresses listed on cover page 4

at the price of B.Fr. 60.—

**Commission of the
European Communities**
D.G. XIII - C.I.D.
29, rue Aldringen
L u x e m b o u r g

November 1972

This document was reproduced on the basis of the best available copy.

EUR 4863 e

POST-IRRADIATION EXAMINATION OF THE FUEL ROD CART-C1 No. 4
by A. FRIGO, R. KLERSY, K.H. SCHRADER, A. SCHÜRENKÄMPER
(EURATOM) - A. BENVENUTI, G. CAMONA and F. MANTEGA (CISE)

Commission of the European Communities
Joint Nuclear Research Centre - Ispra Establishment (Italy)
Luxembourg, November 1972 - 42 Pages - 25 Figures - B.Fr. 60.—

Post-irradiation examinations on the fuel rod have been carried out. The results are presented in the report. Non destructive gamma-scanning analysis shows a migration of Cs inside the fuel and a more or less homogeneous distribution of the fission products Zr, Nb, Ce-Pr and Ru. Metallographic studies show zirconium hydrides over the whole thickness and oxide layers on the surfaces of the cladding. The welding zone appears perfect. The alteration of the microstructure of the fuel due to the irradiation is shown.

EUR 4863 e

POST-IRRADIATION EXAMINATION OF THE FUEL ROD CART-C1 No. 4
by A. FRIGO, R. KLERSY, K.H. SCHRADER, A. SCHÜRENKÄMPER
(EURATOM) - A. BENVENUTI, G. CAMONA and F. MANTEGA (CISE)

Commission of the European Communities
Joint Nuclear Research Centre - Ispra Establishment (Italy)
Luxembourg, November 1972 - 42 Pages - 25 Figures - B.Fr. 60.—

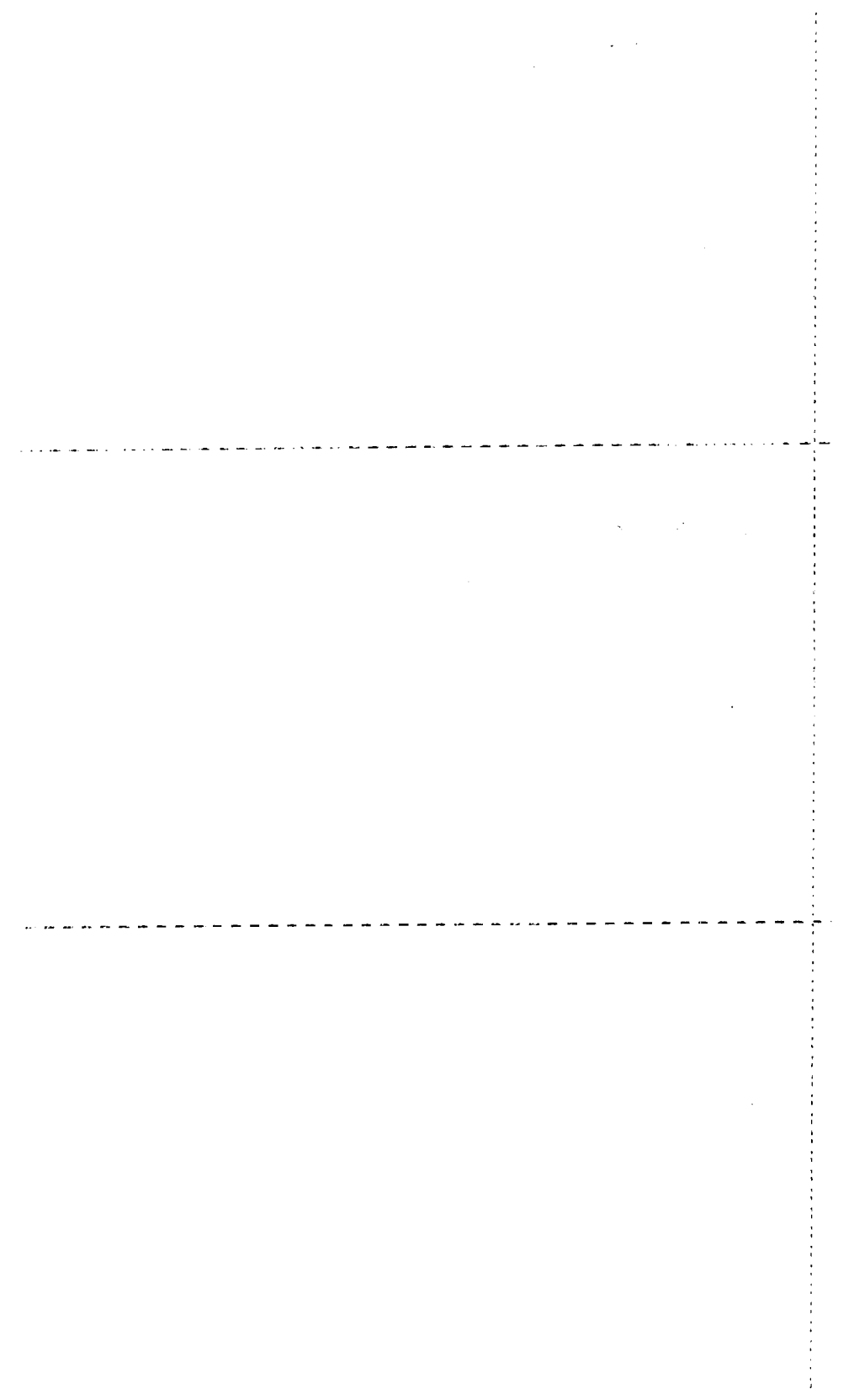
Post-irradiation examinations on the fuel rod have been carried out. The results are presented in the report. Non destructive gamma-scanning analysis shows a migration of Cs inside the fuel and a more or less homogeneous distribution of the fission products Zr, Nb, Ce-Pr and Ru. Metallographic studies show zirconium hydrides over the whole thickness and oxide layers on the surfaces of the cladding. The welding zone appears perfect. The alteration of the microstructure of the fuel due to the irradiation is shown.

EUR 4863 e

POST-IRRADIATION EXAMINATION OF THE FUEL ROD CART-C1 No. 4
by A. FRIGO, R. KLERSY, K.H. SCHRADER, A. SCHÜRENKÄMPER
(EURATOM) - A. BENVENUTI, G. CAMONA and F. MANTEGA (CISE)

Commission of the European Communities
Joint Nuclear Research Centre - Ispra Establishment (Italy)
Luxembourg, November 1972 - 42 Pages - 25 Figures - B.Fr. 60.—

Post-irradiation examinations on the fuel rod have been carried out. The results are presented in the report. Non destructive gamma-scanning analysis shows a migration of Cs inside the fuel and a more or less homogeneous distribution of the fission products Zr, Nb, Ce-Pr and Ru. Metallographic studies show zirconium hydrides over the whole thickness and oxide layers on the surfaces of the cladding. The welding zone appears perfect. The alteration of the microstructure of the fuel due to the irradiation is shown.



EUR 4863 e

COMMISSION OF THE EUROPEAN COMMUNITIES

POST-IRRADIATION EXAMINATION
OF THE FUEL ROD CART-C1 N° 4

by

A. FRIGO, R. KLERSY, K.H. SCHRADER, A. SCHÜRENKÄMPER
(EURATOM)
A. BENVENUTI, G. CAMONA and F. MANTEGA
(CISE)

1972



Joint Nuclear Research Centre
Ispra Establishment - Italy

ABSTRACT

Post-irradiation examinations on the fuel rod have been carried out. The results are presented in the report. Non destructive gamma-scanning analysis shows a migration of Cs inside the fuel and a more or less homogeneous distribution of the fission products Zr, Nb, Ce-Pr and Ru. Metallographic studies show zirconium hydrides over the whole thickness and oxide layers on the surfaces of the cladding. The welding zone appears perfect. The alteration of the microstructure of the fuel due to the irradiation is shown.

KEYWORDS

FUEL RODS	CERIUM 144
RADIATION EFFECTS	PRAESODYMIUM 144
URANIUM DIOXIDE	ZIRCONIUM 95
GAMMA FUEL SCANNING	NIOBIUM 95
FISSION PRODUCTS	MICROSTRUCTURE
DIFFUSION	FUEL CANS
DISTRIBUTION	ZIRCALOY
CESIUM 134	ZIRCONIUM HYDRIDES
CESIUM 137	ZIRCONIUM OXIDES
RUTHENIUM 106	LAYERS

.. TABLE OF CONTENTS *)

	page
1. Fuel rod characteristics and irradiation conditions.	5
2. Non destructive analysis.	7
2.1. Gamma scanning measurements.	7
2.1.1. Total gamma activity measurements.	
2.1.2. Gamma spectrometry.	
2.2. Dimensional measurements.	9
3. Destructive analysis.	10
3.1. Preparation of samples for metallographic studies.	10
3.2. Cladding examination.	10
3.2.1. Zircalov.	10
3.2.2. Zirconium hydrides.	11
3.2.3. Zirconium oxide.	12
3.2.4. Chemical determination of hydrogen content.	12
3.3. Plug examination.	13
3.4. Fuel examination.	13
3.4.1. Grain size.	13
3.4.2. Porosity.	15
3.4.3. Cracks.	15
Acknowledgements.	16

*) Manuscript received on May 23, 1972



1. Fuel rod characteristics and irradiation conditions.

This report deals with postirradiation examinations of rod No. 4 (peripheral) of CART C-1 fuel element central bundle.

Some data of general interest are listed below :

- Rod characteristics

- Cladding - material : Zircaloy-2 reactor grade
- supplier : CEFILAC (Paris)
- nom. size : O.D. : 20 mm
 thickness : 1 mm
- Fuel - material : natural UO₂ in
 synthesized pellets
- manufacturer: FCEC Laboratories
 (pellets) CNEN Saluggia
- nom. size : O.D. : 17.80 mm
 height : 26.00 mm
 dish depth : 1 mm
 (1 per pellet)
- Fuel rod - plug material : Zircaloy-2 reactor
 grade
- filling atmosphere : A 90% - He 10%
 p = 1.1 ÷ 1.2 ata
- manufacturer: FCEC Laboratories
 CNEN Saluggia

- Operative data of the rod

- $\int kdt$ average on the rod : 51.5 W/cm (calculated) with
 temporal peak (about 1 hour)
 at 58 W/cm
- average specific power : nominal 26.7 W/g-UO₂ ; max.
 temporal 30.0 W/g-UO₂
- average burn-up : 1685 MWd/t U

- cooling : water-steam mixture
- coolant pressure and temperature : 50 kg/cm² ; 260°C
- sheath temperature : 270°C
- UO₂ central temperature (calculated) : 2000°C
- number of days in power (higher than 50% of the nominal power) : 80
- number of days in temperature : 110

2. Non destructive analysis.

2.1. Gamma-scanning measurements.

The used apparatus consists of a mechanical part installed inside the hot cell (Fig. 1), a collimator system mounted in the concrete wall of the cell and the equipment for gamma-ray analysis outside the cell. An electronic control unit allows to run measurements automatically following a preselected program for the displacement of the fuel rod and for counting time. In the described experiments the fuel rod was rotating during counting but in a fixed position with regard to the axial direction. A cylindrical collimator with a diameter of 1 mm was used. The total gamma-activity in the energy range from 100 to 2.500 KeV has been measured in steps of 0.5 mm using a NaI-crystal. The gamma-spectre have been measured each 20 mm using a Ge-Li crystal.

2.1.1. Total gamma-activity measurements.

Fig. 2 shows the distribution of the total gamma-activity along the fuel rod. The position of the different fuel pellets inside the rod is indicated. The most significant result is the appearance of significant activity peaks. These peaks correspond to the interfaces of fuel pellets. It must be mentioned that the pellets had a dishing. Very often such a dishing leads to pronounced minima of the measured total gamma-activity. In the present case the contrary has been observed. This is an indication that a transport of fission products from the fuel to the interfaces of the pellets have taken place during irradiation.

The mean value of the gamma-activity shows a slightly increase going from the top to the bottom of the rod. This corresponds to the flux distribution during irradiation. The relatively high scattering of the activity is indicating a cracked fuel.

2.1.2. Gamma-spectrometry.

A spectra of the fission products of the irradiated fuel is shown in fig. 3. The isotopes which have been detected in a significant concentration are given in the table.

<u>Isotope</u>	<u>Gamma-ray energy</u> (KeV)		<u>Half life</u> (days)
Ru 106	512	622	372.5
Cs 134	605	796	749
Cs 137	662		10.990
Ce-Pr 144	696		285
Zr 95	724	756	65
Nb 95	766		35.1

The surface area of an observed peak is roughly proportional to the quantity of the corresponding isotope, which is present in the section under examination. This is only an approximation because different radial distribution of the fission product could lead to different surface areas due to the self adsorption of the X-rays inside the fuel rod itself.

The spectra of the fig. 3 has been measured in the center of a fuel pellet. Fig. 4 shows a spectra measured in a position corresponding to the interface of two pellets. (This position is indicated by A in the figures 5 and 6). It can be seen, that the activity of the Cs 137 and of the Cs 134 is increased in comparison with the other isotopes at the interface of two pellets. In the figures 5 and 6 the distribution of the concentration of the measured isotopes in the fuel rod is plotted together with the total activity. As already mentioned for the total gamma-activity the mean values of the activities of the single

isotopes show also a little increase going from the top to the bottom of the rod. For the isotopes Cs 137 and Cs 134 one observes a high scattering of the measured activities and especially a significant increase of these activities at the interfaces of the fuel pellets. This is not the case for the other fission products.

2.2. Dimensional measurements.

The maximum and minimum diameter of the fuel rod has been measured in three axial positions: in the middle of the rod and at 50 mm distance from the end plugs. A micrometer was used for these measurements. The results are listed in the table below. The corresponding values before irradiation are written in brackets.

POSITION 1 (50 mm from the marked plug)		POSITION 2 (center of the rod)		POSITION 3 (50 mm from the non marked plug)	
min	max	min	max	min	max
mm					
20,100	20,120	20,075	20,130	20,090	20,135
[20,083]	[20,100]	[20,076]	[20,108]	[20,072]	[20,102]

The length of the rod, measured between the plane surfaces of the two plugs, was 487.56 ± 0.02 mm.

3. Destructive analysis.

3.1. Preparation of samples for metallographic studies.

Metallographic analysis has been carried out on 7 samples. The location of these samples in the fuel rod is shown in Fig. 7. For the examination of the cladding (samples 5-6-7) the uranium dioxide has been removed mechanically. The samples were then embedded in copper bakelite mixed resin and submitted to metallographic operations (grinding, polishing, chemical etching) to make visible the zirconium oxide layer, the zircaloy morphology and the presence and the orientation of zirconium hydrides. The same metallographic operations have been carried out with the plug (sample 2) of the fuel rod, in order to investigate in addition to the zircaloy properties the welding zone.

The samples 1,3,4 assigned for the fuel examination have been impregnated superficially with epoxy resin to avoid the loss of fuel fragments during metallographic handling. From the samples 8,9,10 the uranium dioxide has been removed. Using the remaining rings, the hydrogen content of the cladding material has been determined.

3.2. Cladding examinations.

3.2.1. Zircaloy.

The microstructure of the Zircaloy has been observed on samples 5,6,7 on the whole cladding thickness and on the whole circumference. The figures 8,9,10 show the typical microstructure of the external, the middle and the internal zones of the cladding. Excluding the regions extremely close to the surfaces an average grain size of 8.5 - 9 ASTM has been estimated. The microstructure of the middle region is slightly different from the microstructure of the adjacent regions. This was observed for each of the three specimens.

Especially the external zones (Fig. 8a, 9a, 10a) show highly deformed grains with considerable twinning and internal stresses due to the mechanical working. The middle zone (Fig. 8b, 9b, 10b) shows a more homogeneously arranged grain structure with appearance of some twins. Comparing equal zones of different samples one can observe that the grains structure is better developed in the samples 5 and 6 than in the sample 7. This is demonstrated if one compares fig. 8c with fig. 10c or fig. 9b with fig. 10b. There is no evidence that these differences are due to the cladding fabrication.

3.2.2. Zirconium hydrides.

The examination of the zirconium hydrides has been carried out on samples 5,6,7 after polishing and specific etching. The figures 11, 12 and 13 show for each of the three samples two complete radial zones of the cladding. The angle between the two zones is about 90° . The micrographs are representative for the overall structure of each sample. The distribution of the hydride is not uniform. There is a high concentration on the external surface. The concentration is decreasing up to a deepness of $85 - 100 \mu$ and is rather constant in the remaining region. The hydrides have generally the form of needles, which are long and thick in the external region and somewhat smaller than in the other regions of the samples. Considering the needles with a length of more than 5μ , the following numbers per mm^2 have been measured :

- sample 5 : 3470
- sample 6 : 2760
- sample 7 : 2950

Furthermore the number of needles with an inclination smaller than 40° relative to the radius has been determined in order to calculate the orientation factor f_n .

The results are given in the table below.

	Sample 5		Sample 6		Sample 7	
	f_n	fig.	f_n	fig.	f_n	fig.
First radial zone	0.44	11a	0.30	12a	0.43	13a
Second radial zone	0.31	11b	0.31	12b	0.27	13b

The values are especially high in all examined regions. It should be noted that for one sample, that means in one cross section, different values were obtained for different radial zones of the cladding.

3.2.3. Zirconium oxide.

A zirconium oxide layer has been observed on the external surface of the cladding. (fig. 14 and 15). This band of oxide was found on the whole periphery and its thickness is between 4.5μ and 8μ . The most frequent value measured was about 6μ and from a large number of measurements an average value of 6.1μ has been determined for both samples 6 and 7. On both samples some oxide layers have been observed on the inner surface of the cladding (fig. 16 and 17). About 20% of the circumference was covered with oxide. The average value of the thickness was 3.5μ with extreme values of 2.5μ and 4.5μ .

3.2.4. Chemical determination of hydrogen content.

The hydrogen content of the cladding has been determined using the samples 8,9,10. Two measurements have been carried out on each sample.

The mean values are given below :

ring 8	54.6	H ₂ (ppm)
ring 9	73.3	"
ring 10	61.8	"

3.3. Plug examination.

The region of the plug has been examined in order to check the plug-cladding junction and to get information on the microstructure of the region near the welding zone.

Fig. 18a shows the welding zone of the plug in polarized light. The junction appears perfect. The interface of the two original pieces can be recognized due to the presence of small needle shaped grains. In bright field observation no interface at all could be detected (fig. 18b).

The variation of the microstructure of the welding zone can be considered as normal. The interface between the normal grain structure of the cladding and the Widmannstätten structure is rather sharp (fig. 19a). Going to the region of the highest temperature grain size increases more continuously (figures 19b, 19c).

3.4. Fuel examination.

3.4.1. Grain size.

Four typical regions could be found on all samples (1,3,4). Starting from the periphery and going towards the centre of the fuel rod, we observe :

- a first region where the annealing during irradiation led to a sintering without secondary recrystallisation ;
- a second region with grain growth, which occurred in a more or less orientated way ;

- a third region with secondary recrystallisation, which led to large columnar equi-orientated grains ;
- a fourth region with large columnar grains, which are radially orientated.

Differences between different samples consist only in the depth of the typical regions. The mean values are given in the following table, indicating also the reference figures, which show the microstructure.

	Sample 1		Sample 3		Sample 4	
	Depth (mm)	Fig.	Depth	Fig.	Depth	Fig.
1. zone	2.9	20a,b	2.8	21a	3.25	22a,b
2. zone	0.2	20c	0.5	21b	0.15	22b
3. zone	0.35	20c	0.6	21c	0.11	22c
4. zone	5.6	-	5.1	21d	5.2	22d

Fig. 23 shows the microstructure of the sample 3 over the whole section. From the table one can see that the diameter of the region with the columnar grain is decreasing going from sample 1 to sample 3 and 4.

It should be mentioned that only the external zone of the first region shows a microstructure which has practically the same characteristics as the original sintered material (figures 20a, 22a), whilst the zone near the interface with the second region shows a well arranged and defined grain structure (20b, 21a, 22b).

3.4.2. Porosity.

The porosity looks different for the different regions of the fuel section, but there is no difference between the three samples. In the external zone of the first region the fuel shows macroporosity and microporosity, as demonstrated in the figures 20a and 22a. Some of the pores have a size equal to the grain size, others are fixed and limited to grain boundaries (fig. 24a, 24b). In the adjacent zone of the first region macroporosity decreases in quantity, whereas the porosity on the grain boundary is still present. In the second region pores appear rather spherical, mainly fixed on grain boundaries (fig. 24d). Only a few pores have been detected inside the grains. In the third and fourth regions pores, definitely spherical, are more and more aligned at grain boundaries as the fuel center is approached (fig. 22c, 23).

3.4.3. Cracks.

Fig. 25 shows a typical example of the cracked fuel. In the external region one observes radial and circumferential cracks. In the adjacent region up to the fuel center, micro- and macrocracks appear. They are partially intergranular and show always a radial direction.

ACKNOWLEDGEMENTS

The Authors wish to thank Mr. Buscaglia G., Mr. Ghezzi E., Mr. Parisotto A., for their help in samples preparation and metallographic examinations.

LIST OF FIGURES

- Fig. 1 Gamma-scanning equipment.
- Fig. 2 : Total gamma activity.
- Fig. 3 : Typical gamma spectrum of the fuel.
- Fig. 4 : Gamma spectrum measured on the interface
between two pellets.
- Fig. 5 : Distribution of Cs 134, Ce-Pr 144 and Ru 106
in the fuel rod.
- Fig. 6 : Distribution of Zr 95 and Cs 137 in the fuel
rod.
- Fig. 7 : Location of samples for post-irradiation
examination.
- Fig. 8 : Zircaloy morphology, sample 5.
- Fig. 9 : Zircaloy morphology, sample 6.
- Fig. 10 : Zircaloy morphology, sample 7.
- Fig. 11(a,b) : Zirconium hydride in two radial zones
(sample 5).
- Fig. 12(a,b) : Zirconium hydride in two radial zones
(sample 6).
- Fig. 13(a,b) : Zirconium hydride in two radial zones
(sample 7).
- Fig. 14(a,b) : Zirconium oxide on the external surface
(sample 6).
- Fig. 15(a,b) : Zirconium oxide on the external surface
(sample 7).
- Fig. 16 : Zirconium oxide on the inner surface
(sample 6).
- Fig. 17 : Zirconium oxide on the inner surface
(sample 7).

List of figures

- Fig. 18(a,b) : Welding zone of the plug
a : polarized light
b : bright field
- Fig. 19(a,b,c) : Heated zone of the plug
(polarized light).
- Fig. 20(a,b,c) : Microstructure of the fuel
(sample 1).
- Fig. 21(a,b,c,d) : Microstructure of the fuel
(sample 3).
- Fig. 22(a,b,c,d) : Microstructure of the fuel
(sample 4).
- Fig. 23 : Metallographic structure of fuel rod
section.
- Fig. 24(a,b,c,d) : Porosity of UO_2 .
- Fig. 25 : Cracked fuel.

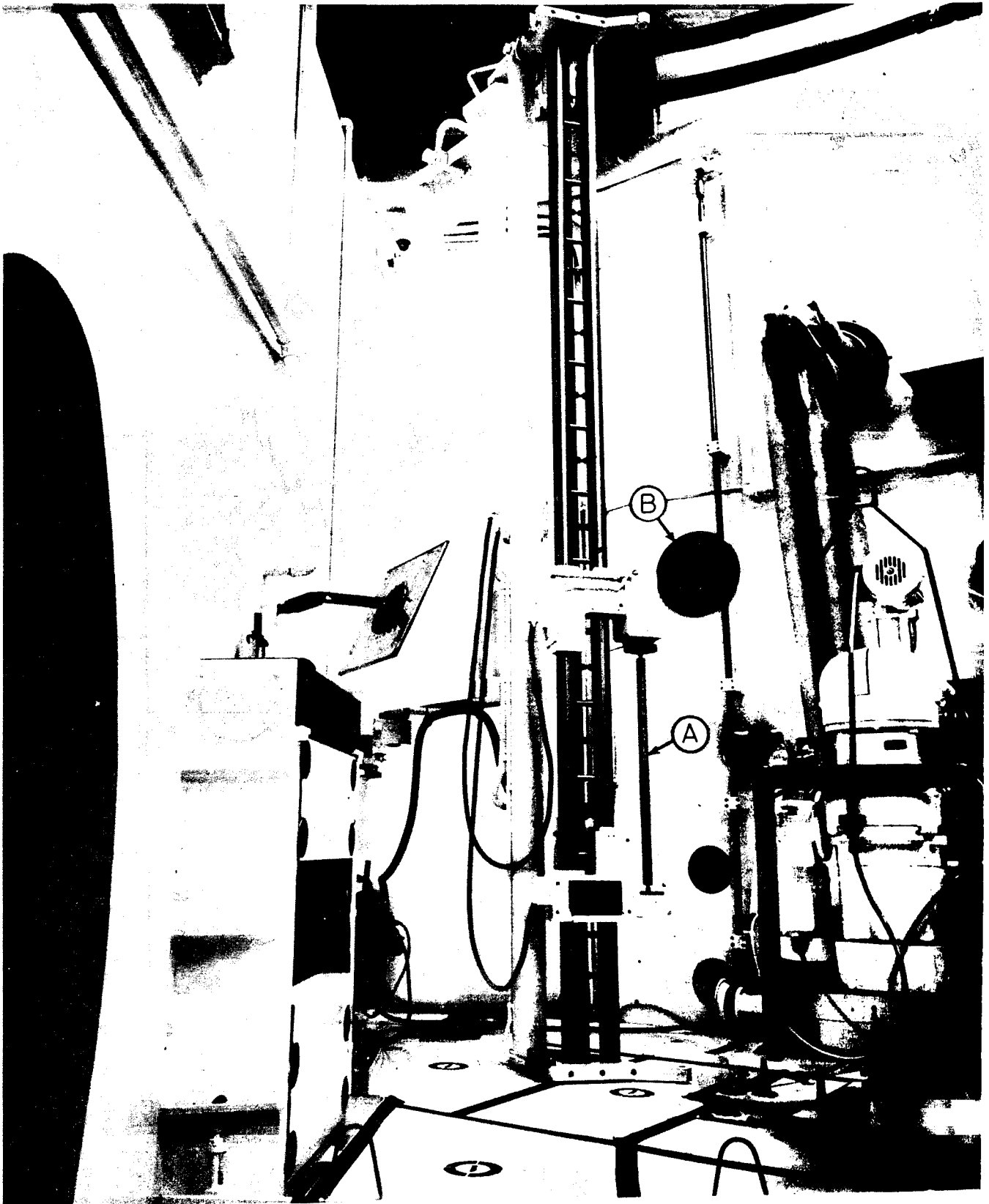


Fig.1 - Gamma-scanning equipment

A : fuel element

B : collimator

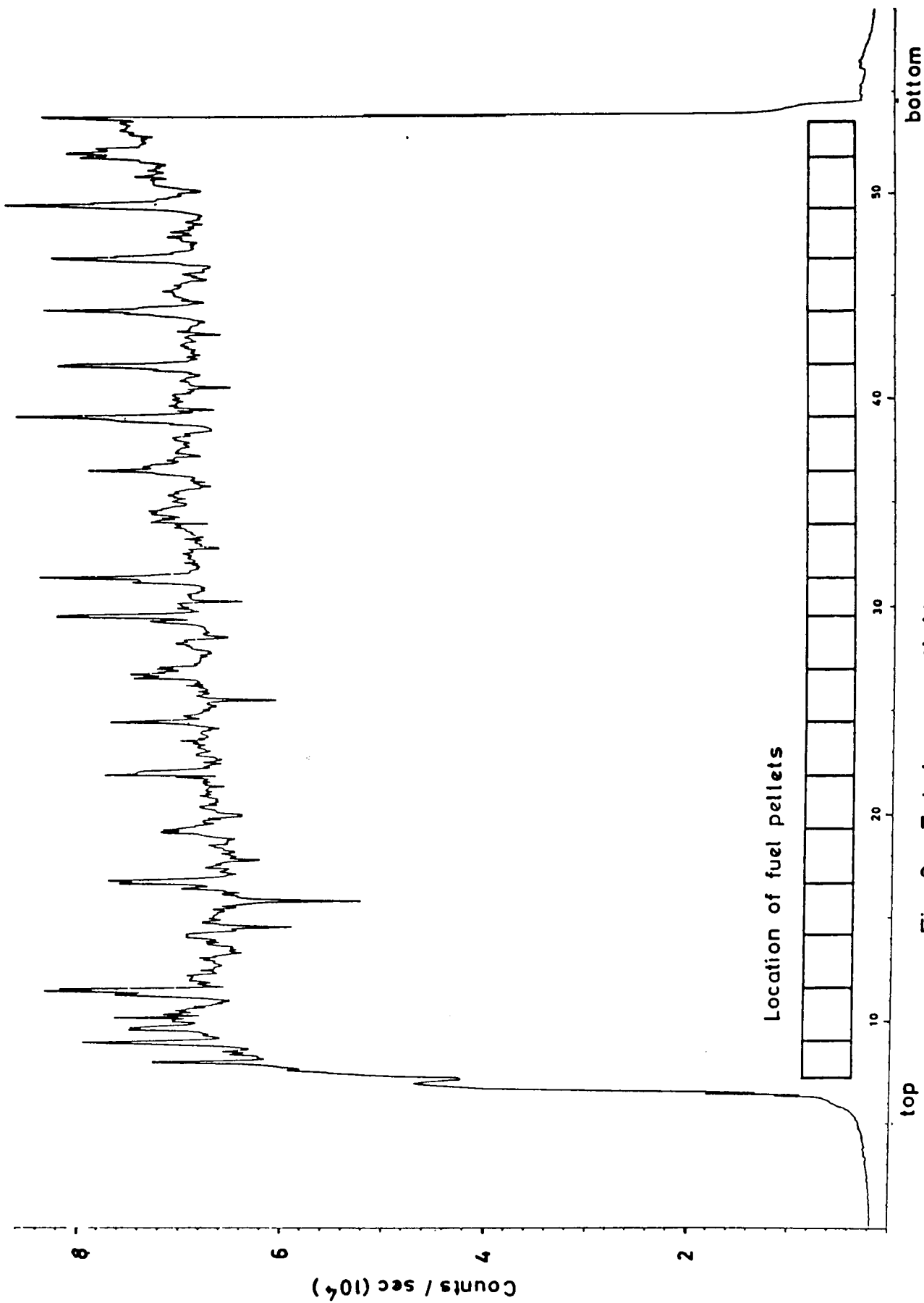


Fig.2 - Total γ -activity

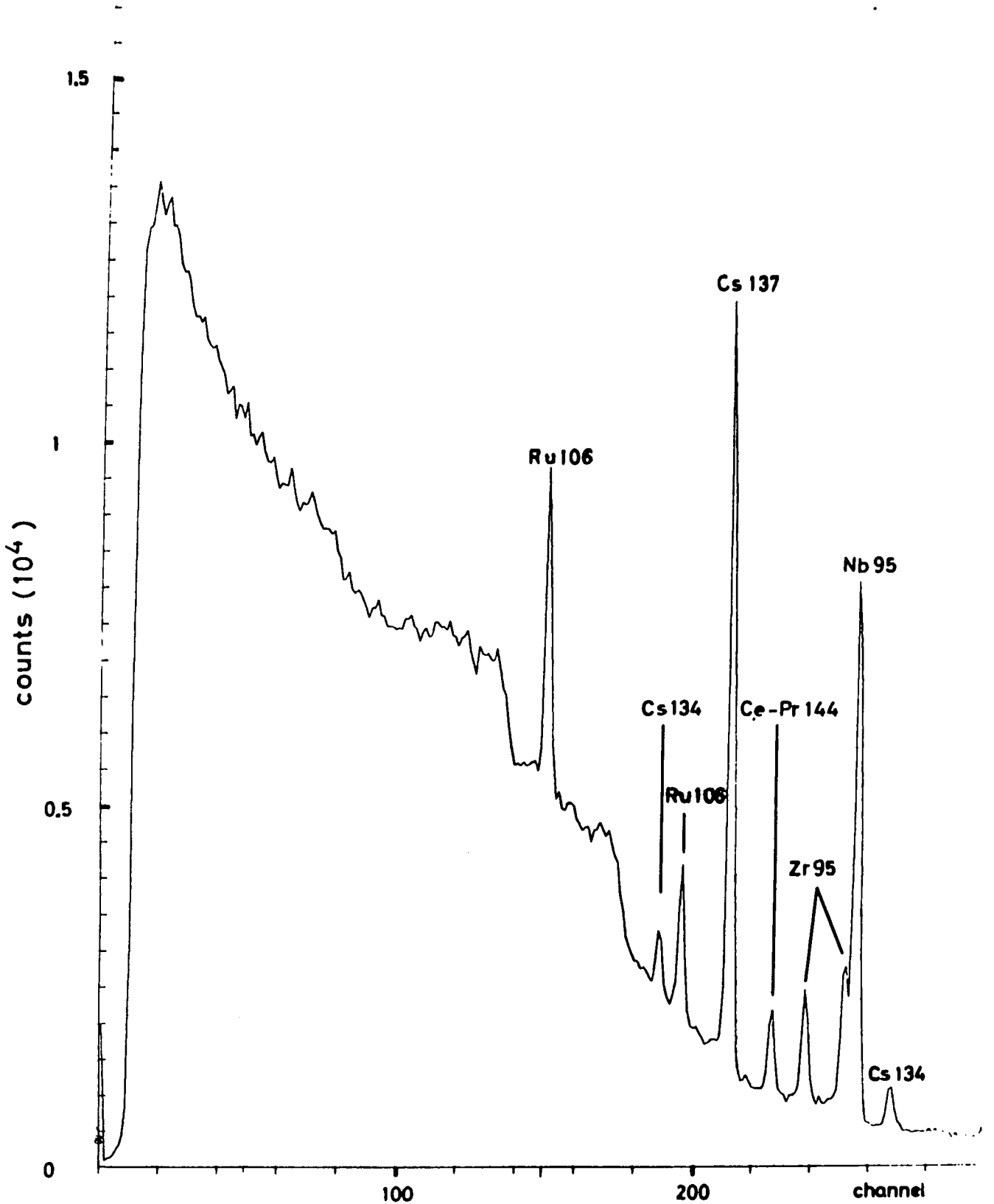


Fig.3 - Typical γ -spectrum of the fuel.

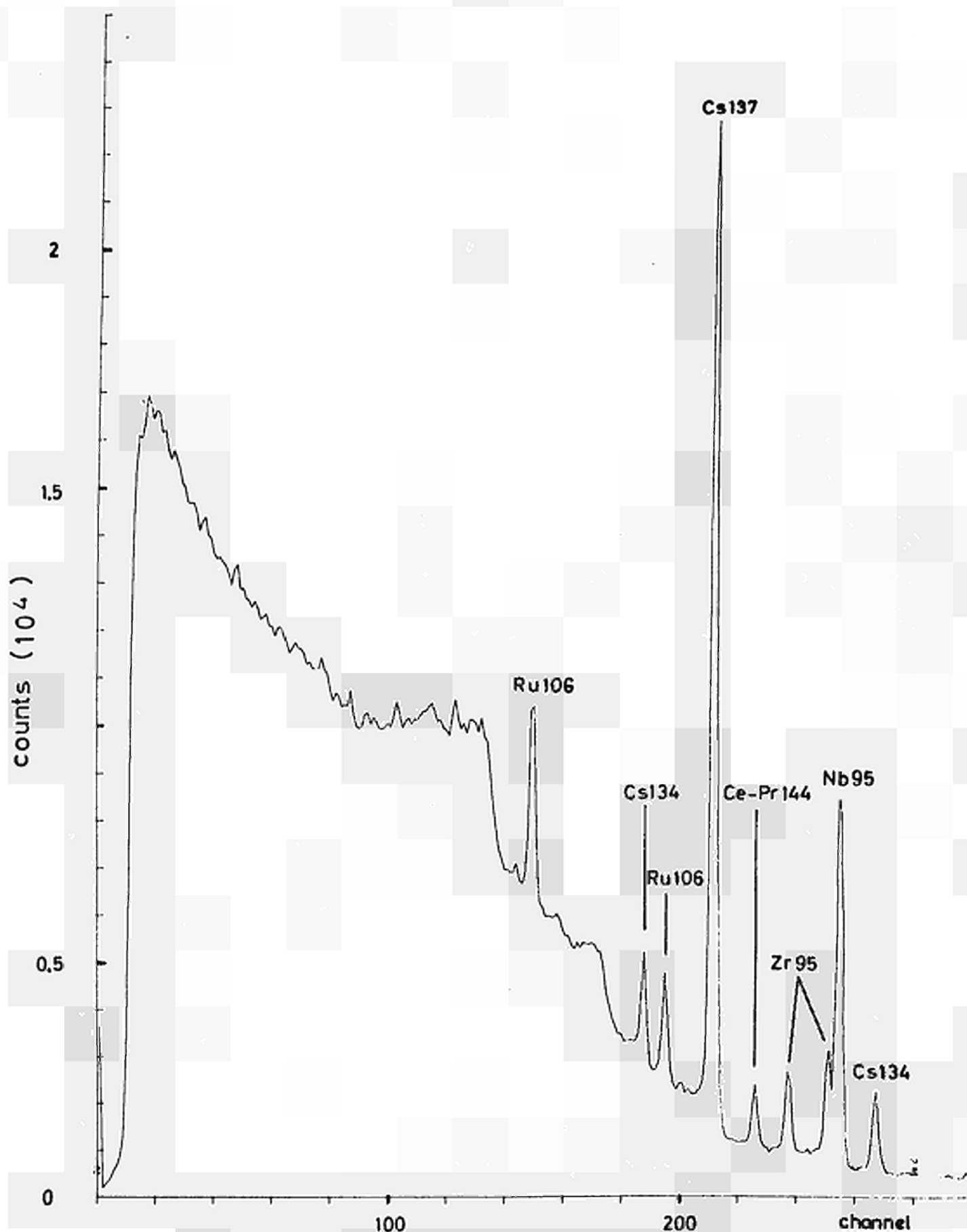


Fig.4 - γ -spectrum measured on the interface of two pellets.

Activity of isotopes counts / min

100
50

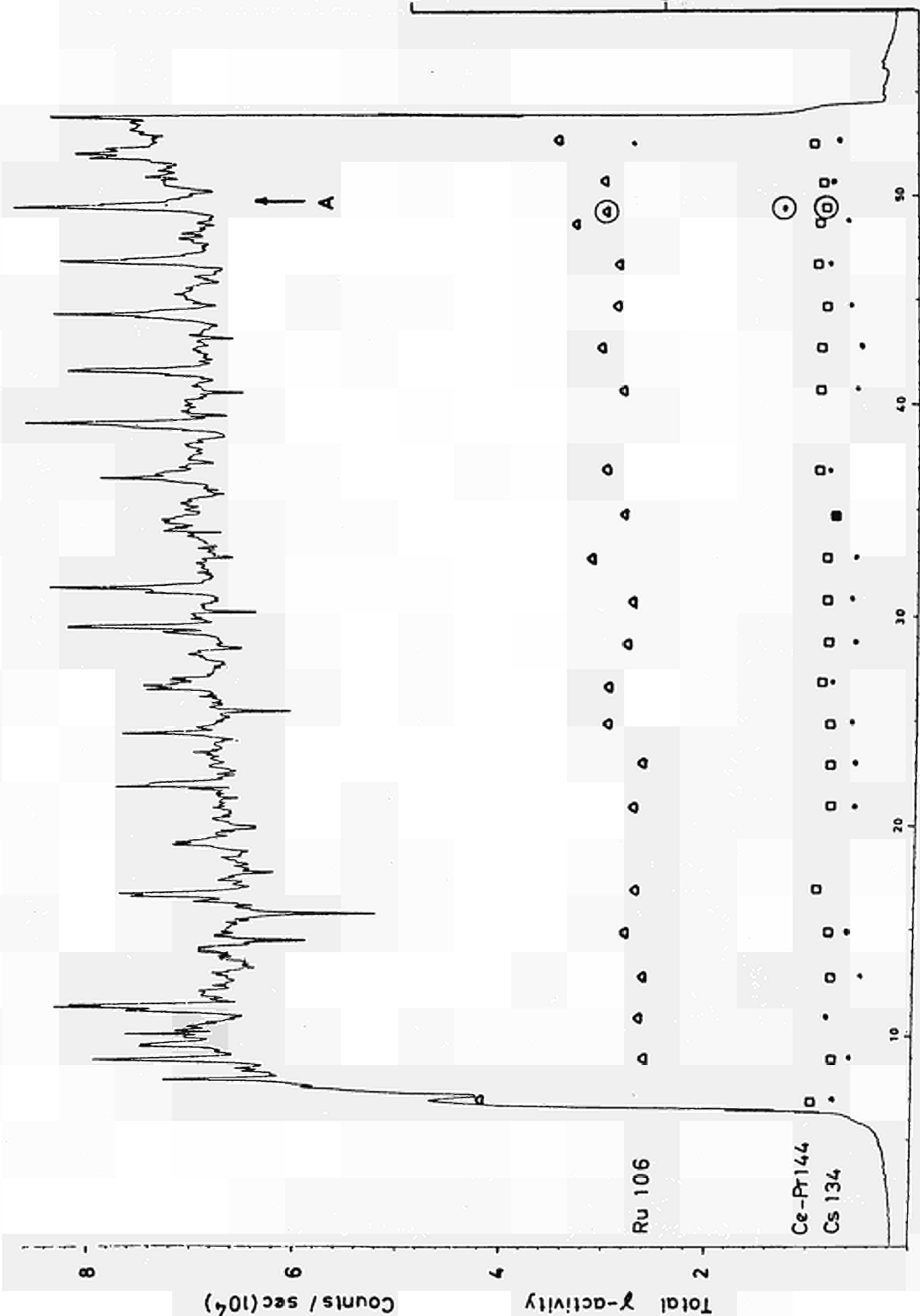


Fig.5 - Distribution of fission product activities.

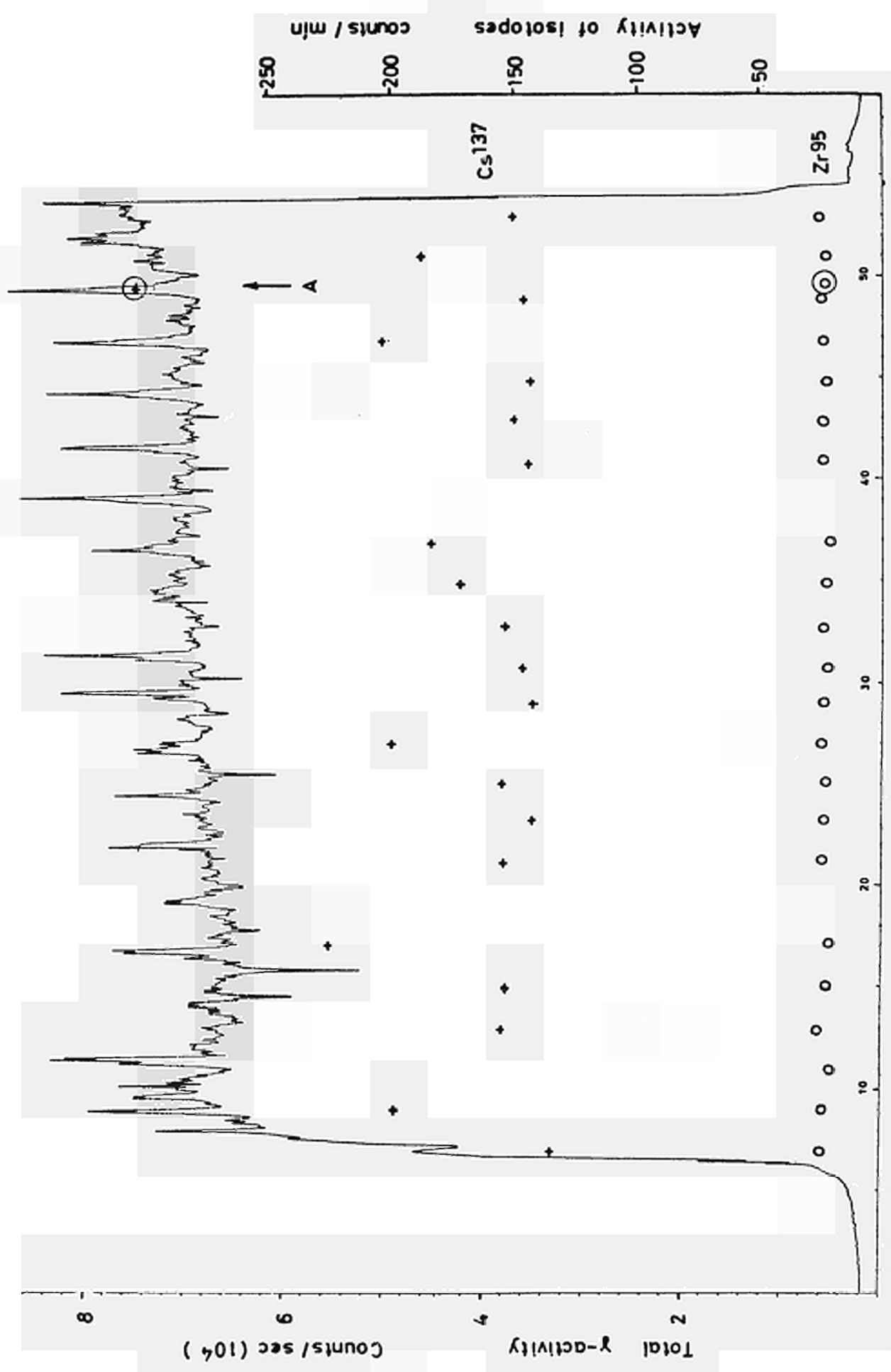


Fig.6 - Distribution of fission product activities.

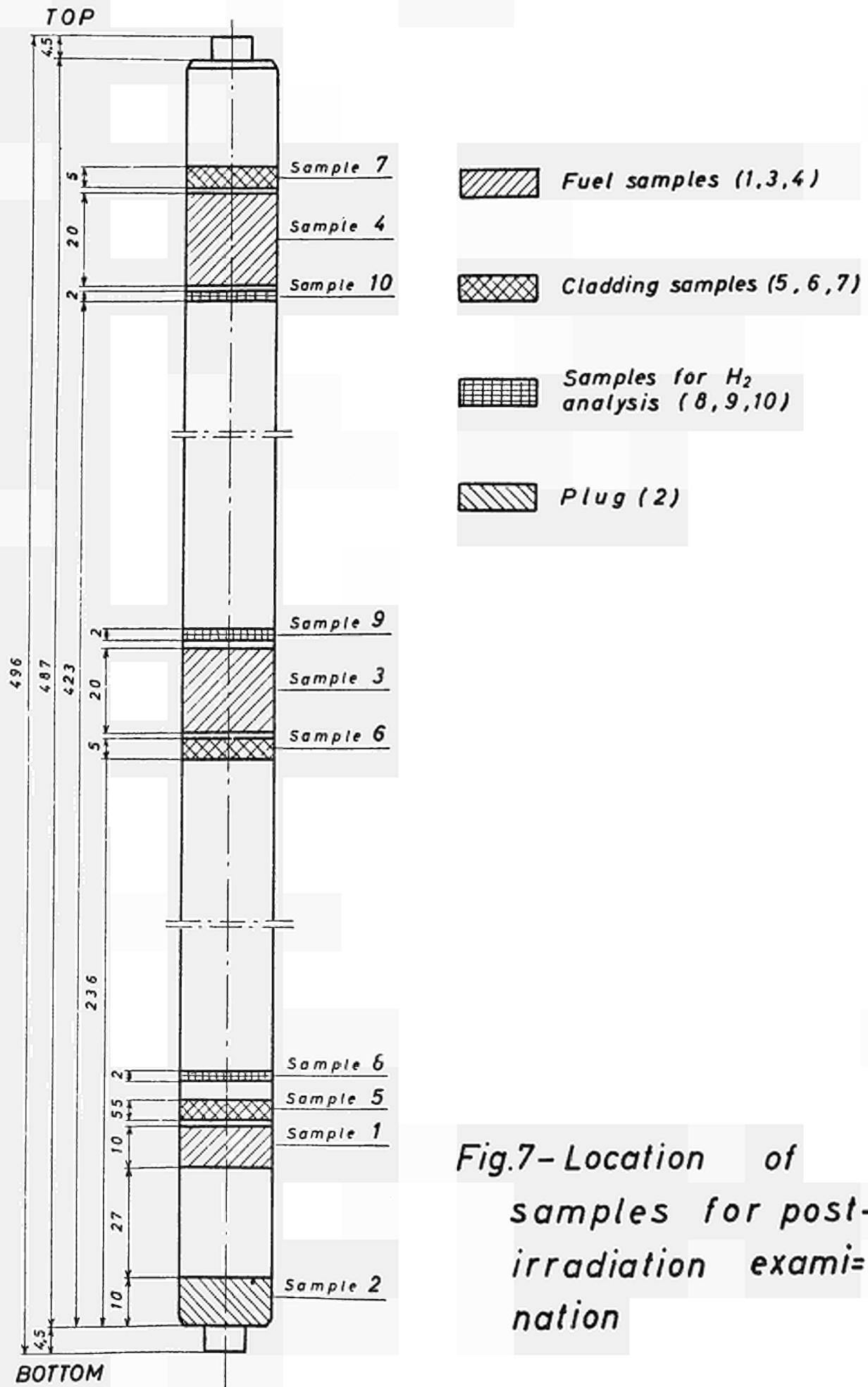
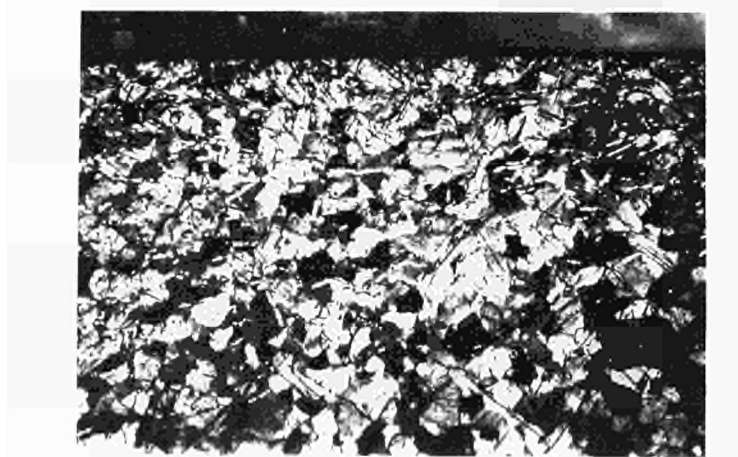
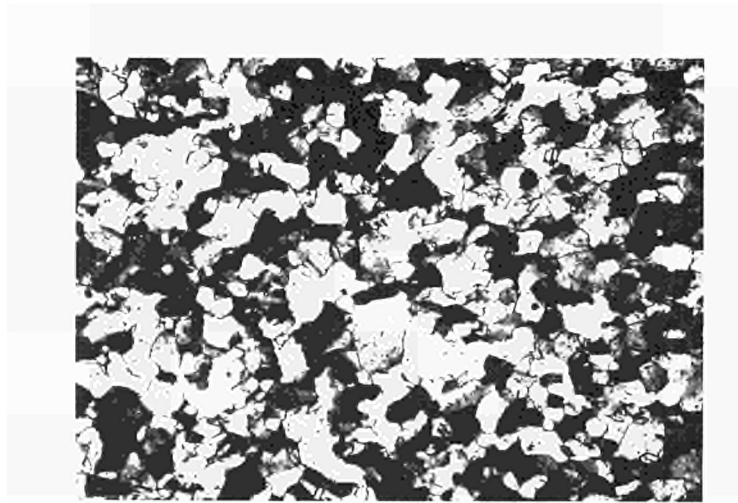


Fig.7- Location of samples for post-irradiation examination



a



b

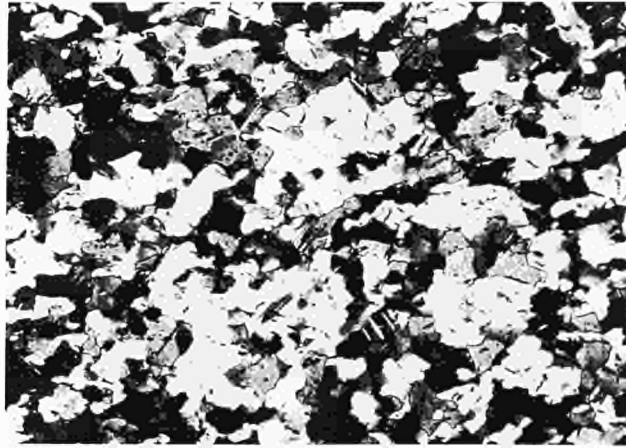


c

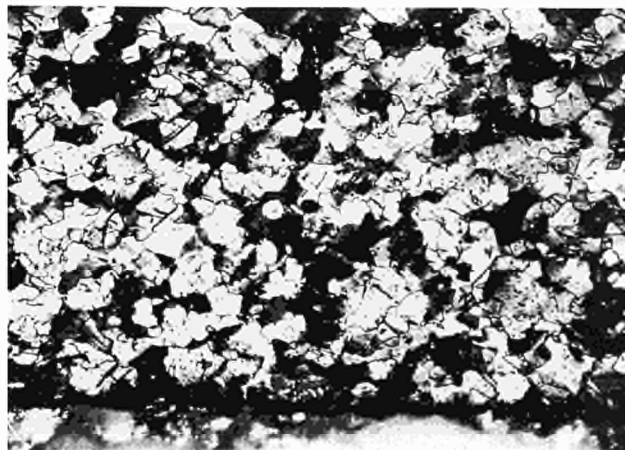
FIG. 8 - Zircaloy morphology (sample 5)
polarized light 200 x



a



b

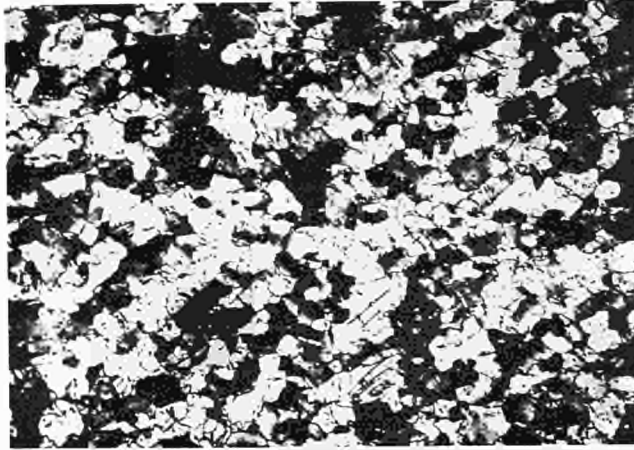


c

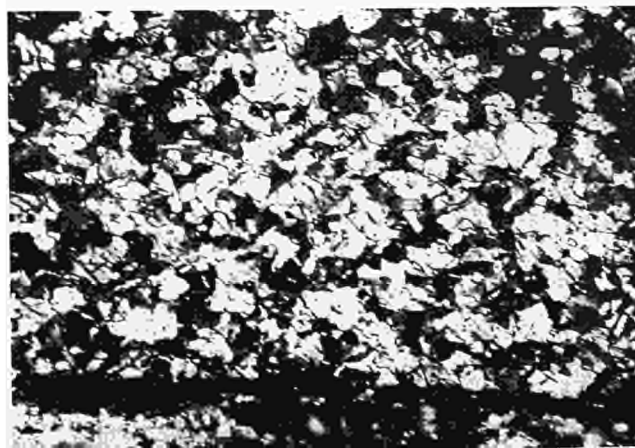
FIG. 9 - Zircaloy morphology (sample 6)
polarized light 200 x



a



b



c

FIG. 10 - Zircaloy morphology (sample 7)
polarized light 200 x

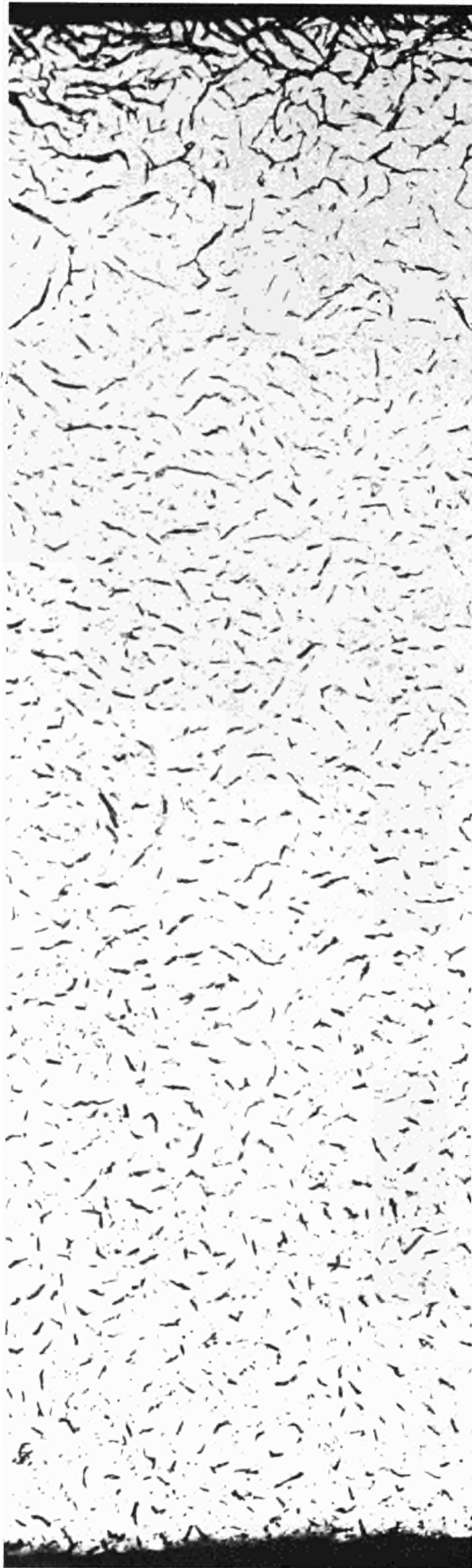


a

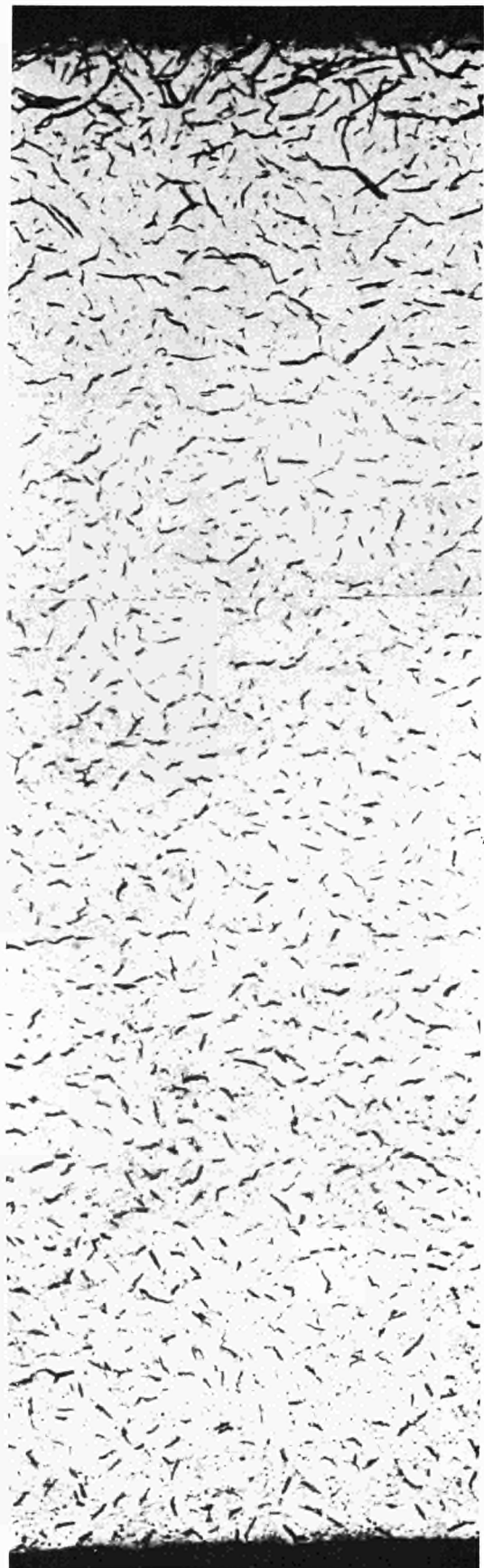


b

FIG. 11 - Zirconium hydride in two radial zones
(sample 5) 250 x



a



b

FIG. 12 - Zirconium hydride in two radial zones
(sample 6) 250 x

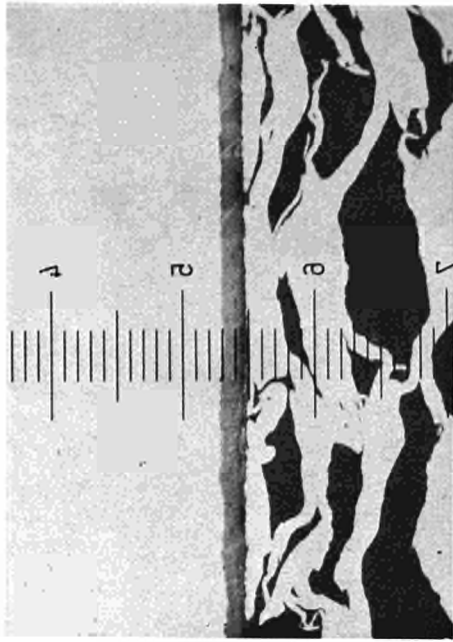


a

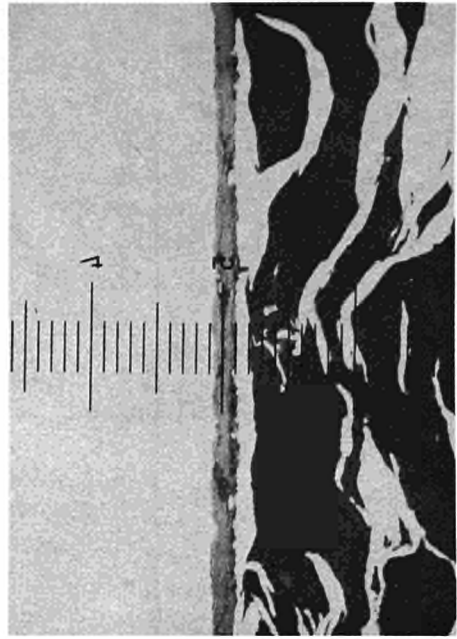


b

FIG. 13 - Zirconium hydride in two radial zones.
(sample 7) 250 x

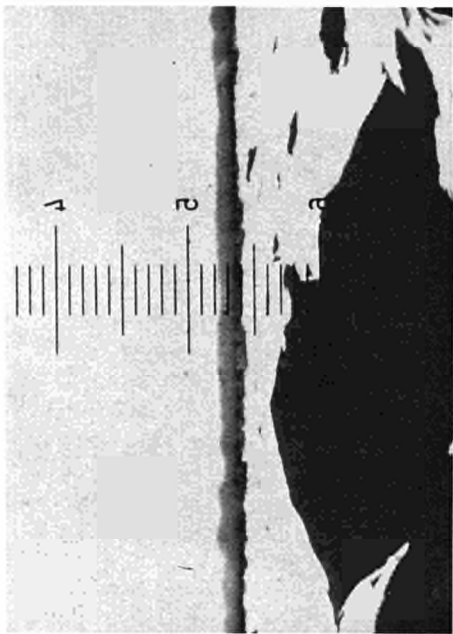


a

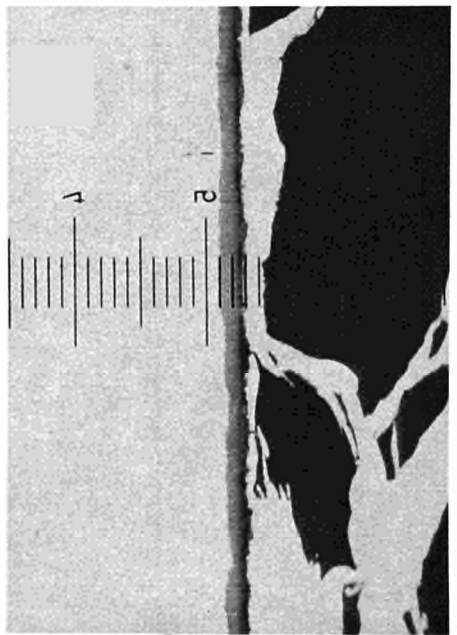


b

FIG. 14 - Zirconium oxide on the external surface.
(sample 6) 460 x



a



b

FIG. 15 - Zirconium oxide on the external surface
(sample 7) 460 x

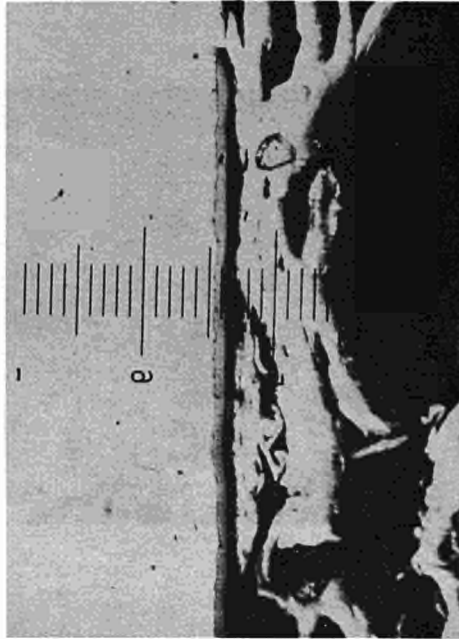


FIG. 16 - Zirconium oxide on the inner surface.
(sample 6) 460 x

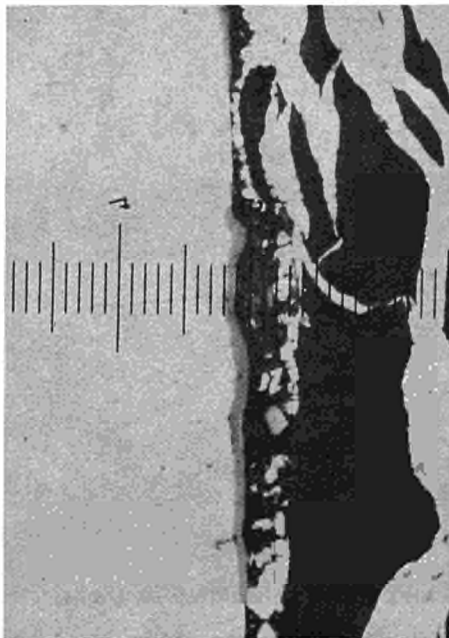
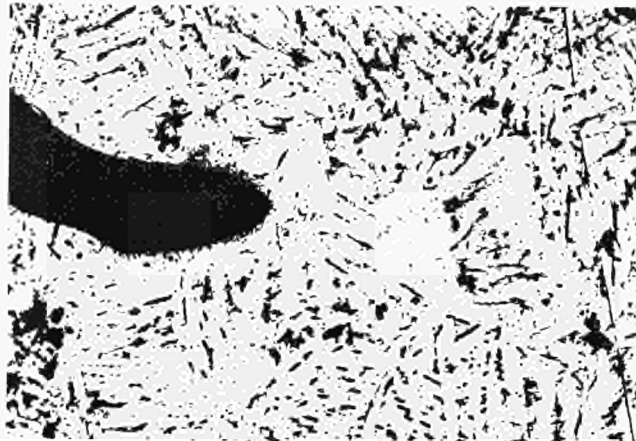


FIG. 17 - Zirconium oxide on the inner surface.
(sample 7) 460 x



a

32 x



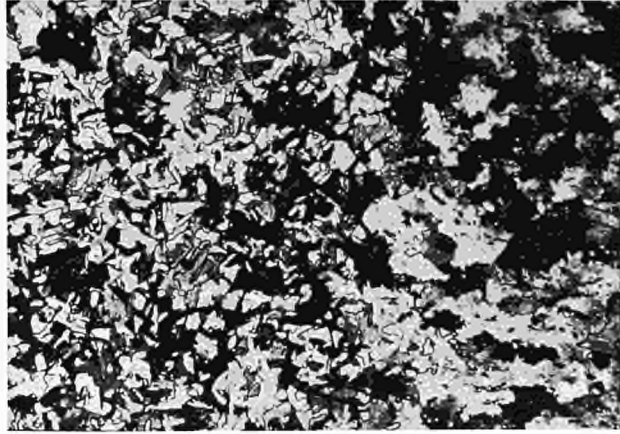
b

200 x

FIG. 18 - Welding zone of the plug.

a : polarized light

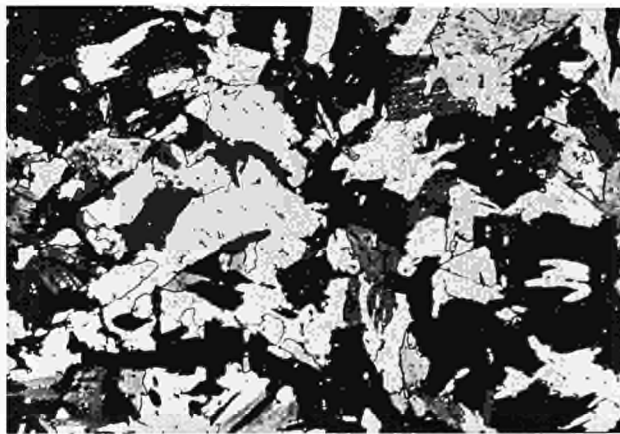
b : bright field



a

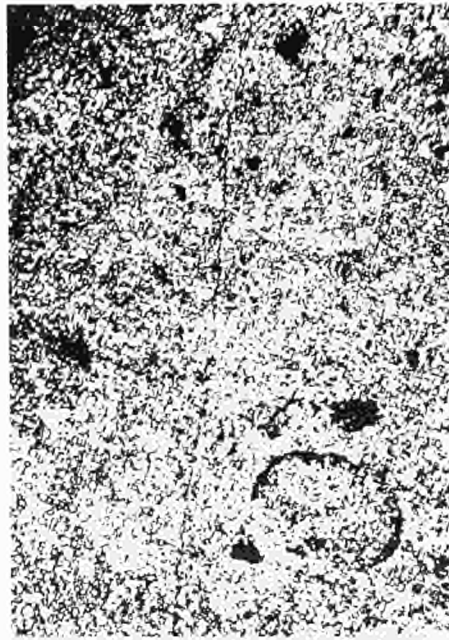


b

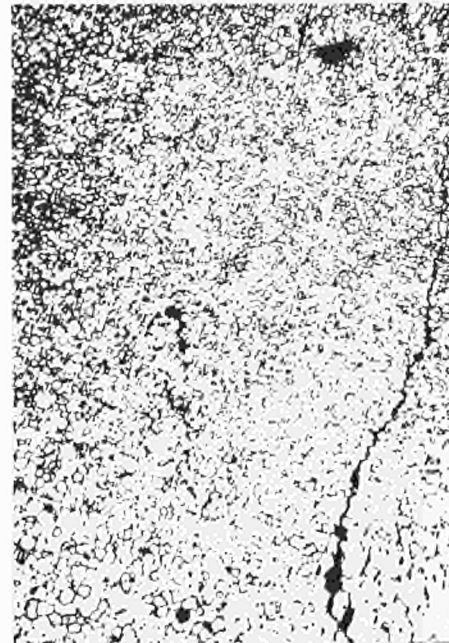


c

FIG. 19 - Heated zone of the plug.
(polarized light)
200 x



a

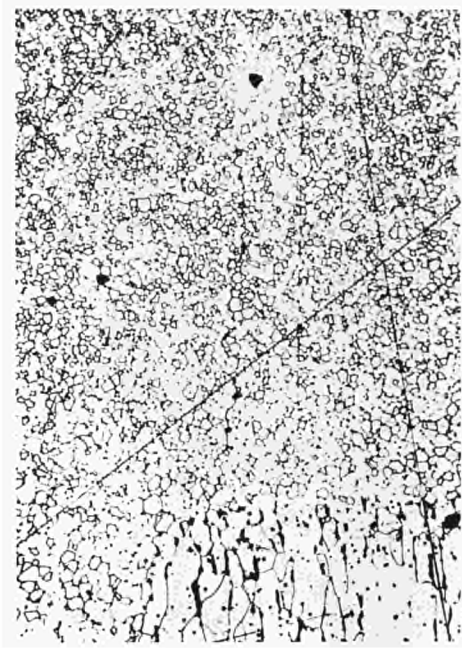


b

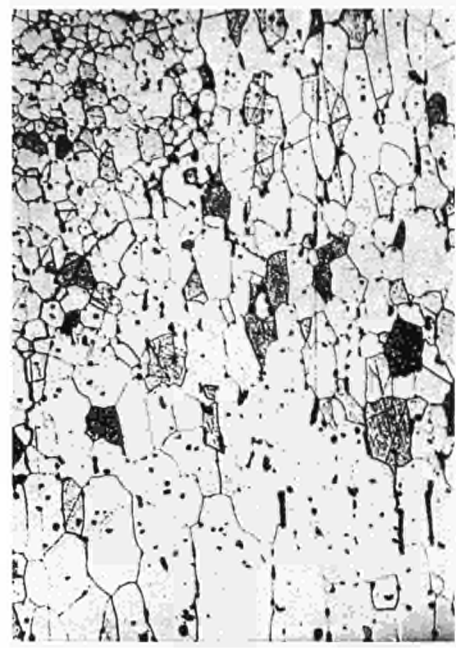


c

FIG. 20 - Microstructure of the fuel (sample 1) 128 x



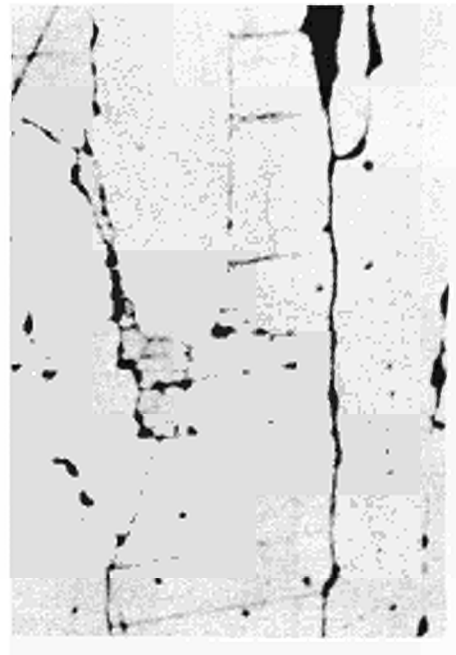
a



b



c

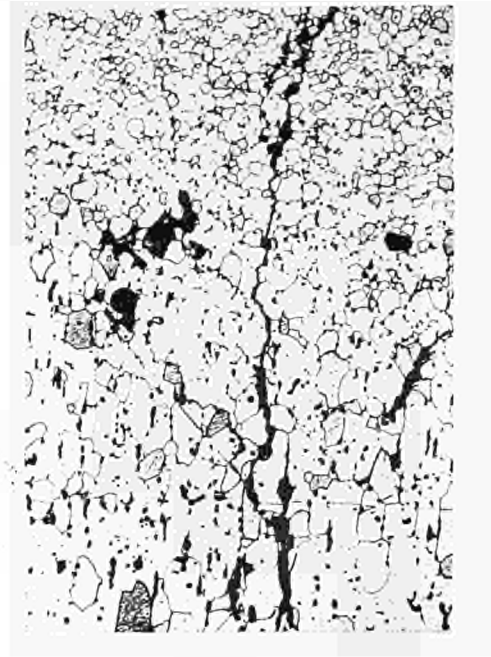


d

FIG. 21 - Microstructure of the fuel
(sample 3) 128 x



a



b



c



d

FIG. 22 - Microstructure of the fuel.
(sample 4) 128 x

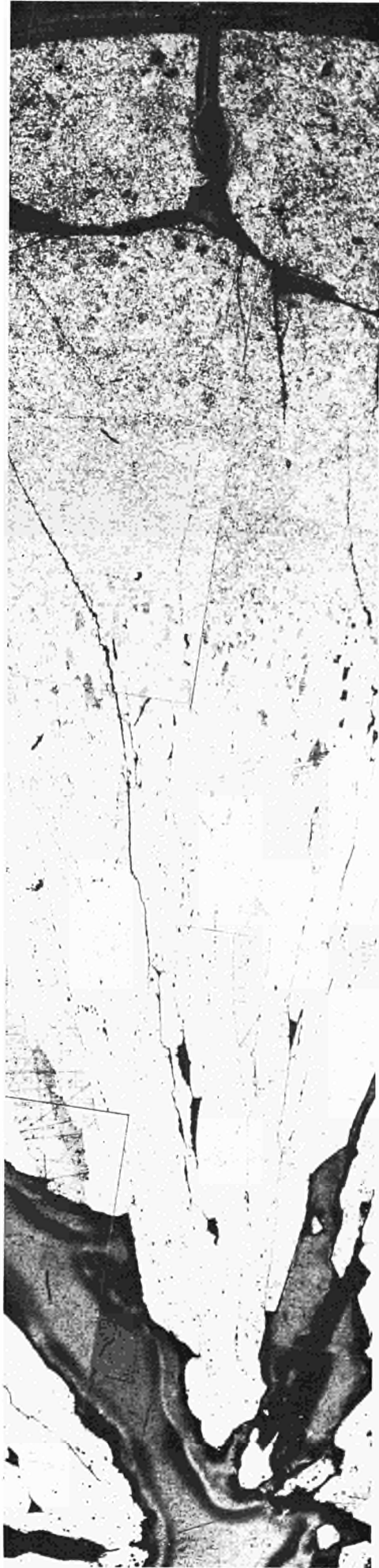
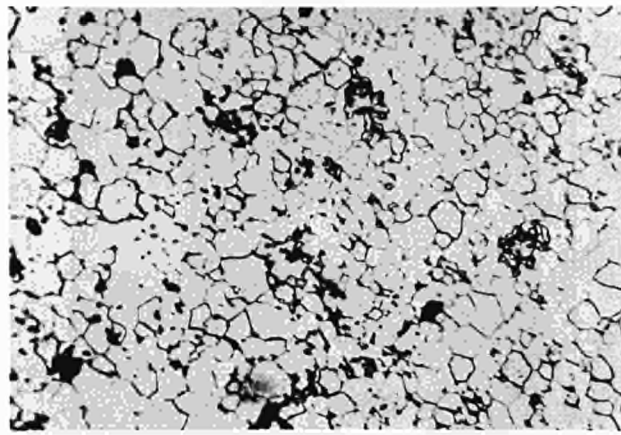
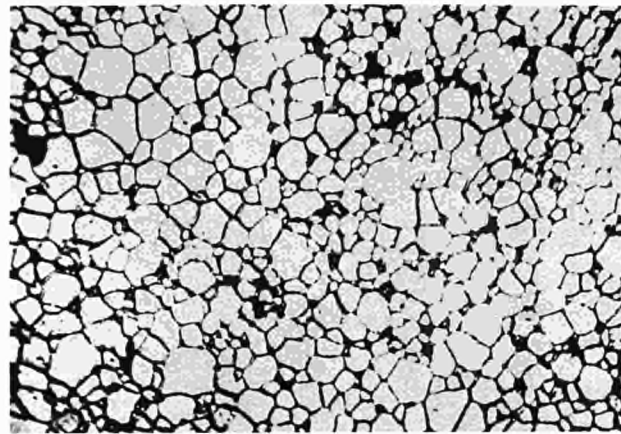


FIG.23 —Metallographic structure of fuel rod section.

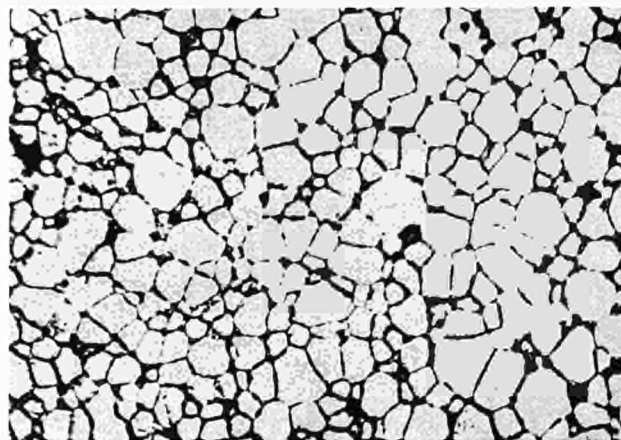
32 x



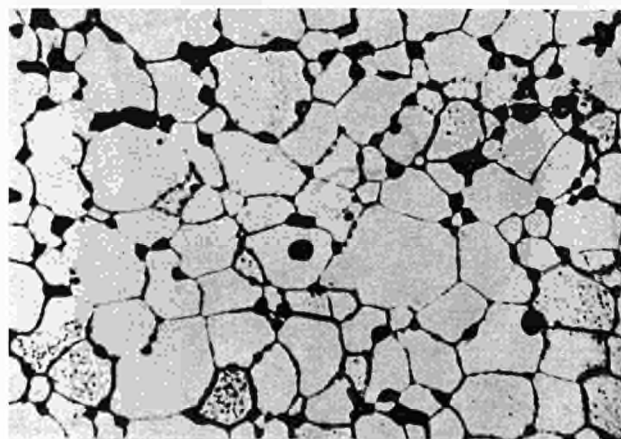
a



b



c



d

FIG. 24 - Porosity of UO_2 .
625 x

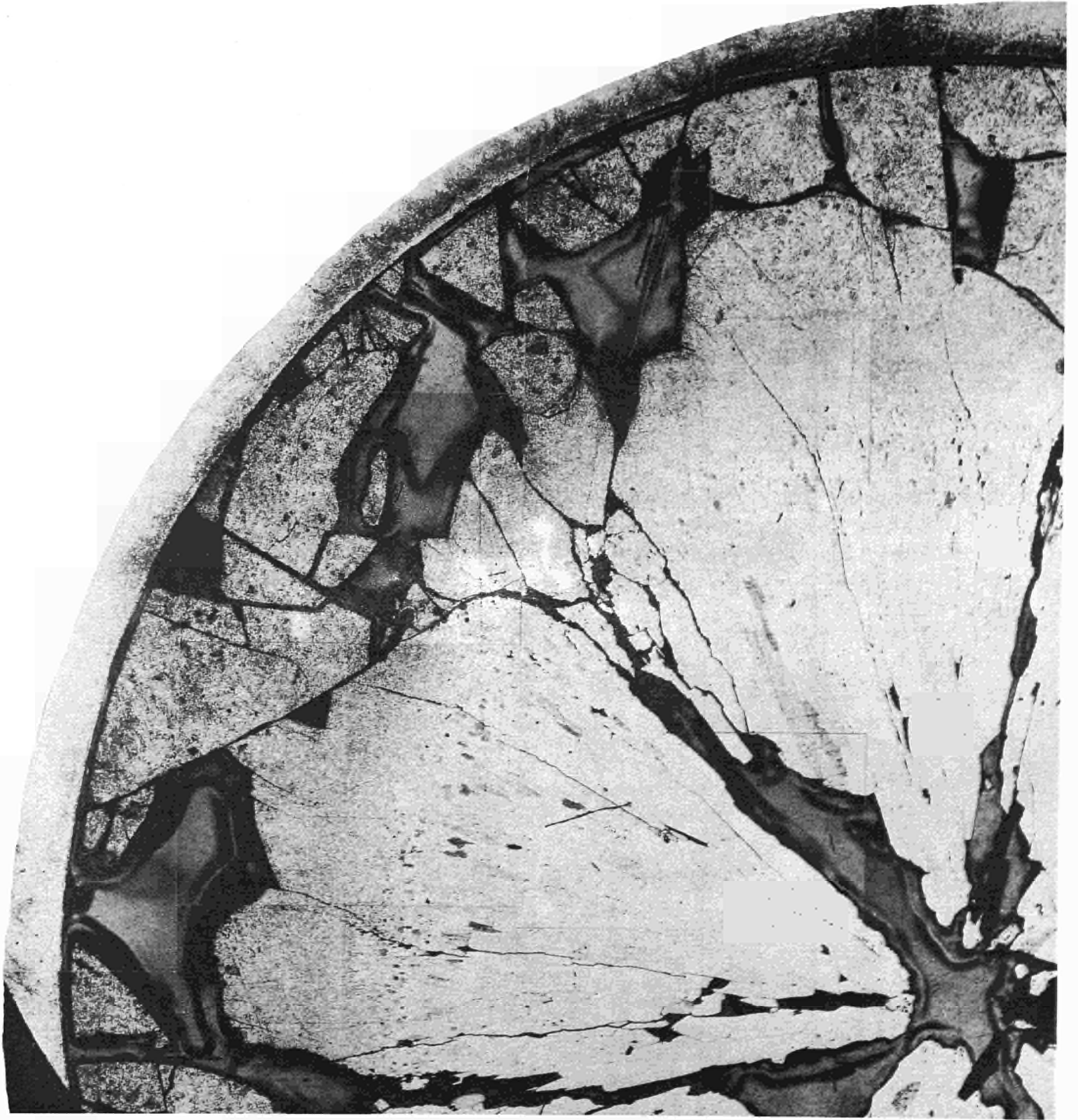


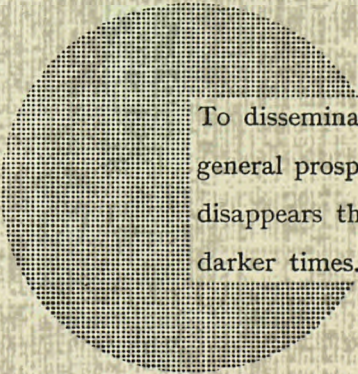
FIG. 25 - Cracked fuel.



NOTICE TO THE READER

All scientific and technical reports published by the Commission of the European Communities are announced in the monthly periodical "euro-abstracts". For subscription (1 year: B.Fr. 1 025,—) or free specimen copies please write to:

**Office for Official Publications
of the European Communities
Case postale 1003
Luxembourg 1
(Grand-Duchy of Luxembourg)**



To disseminate knowledge is to disseminate prosperity — I mean general prosperity and not individual riches — and with prosperity disappears the greater part of the evil which is our heritage from darker times.

Alfred Nobel

SALES OFFICES

The Office for Official Publications sells all documents published by the Commission of the European Communities at the addresses listed below, at the price given on cover. When ordering, specify clearly the exact reference and the title of the document.

GREAT BRITAIN AND THE COMMONWEALTH

H.M. Stationery Office
P.O. Box 569
London S.E. 1

UNITED STATES OF AMERICA

European Community Information Service
2100 M Street, N.W.
Suite 707
Washington, D.C. 20 037

BELGIUM

Moniteur belge — Belgisch Staatsblad
Rue de Louvain 40-42 — Leuvenseweg 40-42
1000 Bruxelles — 1000 Brussel — Tel. 12 00 26
CCP 50-80 — Postgiro 50-80

Agency:
Librairie européenne — Europese Boekhandel
Rue de la Loi 244 — Wetstraat 244
1040 Bruxelles — 1040 Brussel

GRAND DUCHY OF LUXEMBOURG

*Office for official publications
of the European Communities*
Case postale 1003 — Luxembourg 1
and 29, rue Aldringen, Library
Tel. 4 79 41 — CCP 191-90
Compte courant bancaire: BIL 8-109/6003/200

FRANCE

*Service de vente en France des publications
des Communautés européennes*
26, rue Desaix
75 Paris-15^e — Tel. (1) 306.5100
CCP Paris 23-96

GERMANY (FR)

Verlag Bundesanzeiger
5 Köln 1 — Postfach 108 006
Tel. (0221) 21 03 48
Telex: Anzeiger Bonn 08 882 595
Postcheckkonto 834 00 Köln

ITALY

Libreria dello Stato
Piazza G. Verdi 10
00198 Roma — Tel. (6) 85 09
CCP 1/2640

Agencies:
00187 Roma — Via del Tritone 61/A e 61/B
00187 Roma — Via XX Settembre (Palazzo
Ministero delle finanze)
20121 Milano — Galleria Vittorio Emanuele 3
80121 Napoli — Via Chiaia 5
50129 Firenze — Via Cavour 46/R
16121 Genova — Via XII Ottobre 172
40125 Bologna — Strada Maggiore 23/A

NETHERLANDS

Staatsdrukkerij- en uitgeverijbedrijf
Christoffel Plantijnstraat
's-Gravenhage — Tel. (070) 81 45 11
Giro 425 300

IRELAND

Stationery Office
Beggar's Bush
Dublin 4

SWITZERLAND

Librairie Payot
6, rue Grenus
1211 Genève
CCP 12-236 Genève

SWEDEN

Librairie C.E. Fritze
2, Fredsgatan
Stockholm 16
Post Giro 193, Bank Giro 73/4015

SPAIN

Libreria Mundi-Prensa
Castello, 37
Madrid 1

OTHER COUNTRIES

*Sales Office for official publications
of the European Communities*
Case postale 1003 — Luxembourg 1
Tel. 4 79 41 — CCP 191-90
Compte courant bancaire: BIL 8-109/6003/200